Time Delay Control with Switching Action using Frequency-Shaped Integral Sliding Surface

Sung-Uk Lee,
Nuclear Robotics Lab.
Korea Atomic Energy Research Institute,
150 Dujin-dong, Yuseong, Daejeon
305-353 Korea
sulee@mecha.kaist.ac.kr

Pyung Hun Chang and Seong-Tae Kim
Dept. of Mechanical Engineering,
Korea Advanced Institute of Science and Technology,
373-1 Kusung-dong, Yuseong, Daejeon
305-701, Korea
phchang@kaist.ac.kr and dreamer@mecha.kaist.ac.kr

ABSTRACT

Recently the Time Delay Control with Switching Action (TDCSA) method has been proposed as a promising technique in the robust control area, where the plant has unknown dynamics with parameter variations and substantial disturbances are present. When TDCSA is applied to nonlinear system having frequency resonances, TDCSA reveals chattering problem or undesired vibration. This undesired vibration and chattering problem come from the switching action and high gains. Fast sliding mode dynamics or fast desired error dynamics improve the control performance, but excite the unmodeled resonance modes and cause undesired vibration or chattering. To solve this problem, we proposed an integral sliding surface design method using frequency-shaping features. This method is to incorporate frequency-shaping LQ design techniques into an integral sliding surface. By experimental results, the frequency-shaped integral sliding surface was shown to be a practicable for a single-link flexible arm. Motion control of a single-link flexible arm with unmodeled flexible modes was taken into account. The desired trajectory was tracked while minimally exciting the unmodeled flexible modes.

1. Introduction

Recently, the Time Delay Control with Switching Action (TDCSA) method [3, 4] has been proposed as a promising technique in the robust control area, where the plant has an unknown dynamics with parameter variations and substantial disturbances are preset. Specifically, TDCSA consists of Time Delay Control (TDC) [8], which estimates the amounts of an unknown nonlinear dynamics and unexpected uncertainties and cancels them, and a switching action [7] based on sliding mode control. The switching action, a discontinuous input used in sliding mode control, keeps a tracking error on predefined sliding surface which matches the desired error dynamics of TDC. Namely, the switching action compensates for the time delay estimation error of TDC and makes the TDC more robust. Its effectiveness has been demonstrated through the successful application to a 21-ton robotic excavator [3] and a DC motor [4].

However, when TDCSA is applied to nonlinear system having high frequency resonance modes which cannot be modeled completely by a rigid body model, *undesired vibration or chattering* is occurred. This problem, which Sliding mode control reveals also, results from the switching action and high gains. More specifically, a flexible manipulator has high frequency resonance modes. If we design fast sliding mode dynamics or fast desired error dynamics to improve the control performance, high frequency control inputs excite resonance modes and may cause undesired vibration or chattering. To avoid this excitation, the sliding mode dynamics or desired error dynamics should have a slow response. A typical method to suppress chattering problem is the introduction of a smoothing function instead of the signum functions. Such a smoothing function, however, lowers the robustness to steady disturbances and a steady error occurs. So, new method is required to eliminate the undesired vibration or chattering.

To solve this problem in sliding mode control, several researchers have studied the sliding surface design method with frequency-shaped cost functional [2, 6, 9]. Gupta [1] proposed frequency-shaping linear quadratic (LQ) design method and applied it to flexible structure control with success. Young and Özgüner [9] have proposed the sliding surface design method using frequency-shaping linear quadratic (LQ) design techniques, which Gupta [2] proposed. In this method, the state space is extended to include an additional observer dynamics. The new state is guided by a linear quadratic regulator (LQR) optimization law to establish certain frequency characteristics for the original dynamics. Therefore, an optimal sliding surface considering unmodeled dynamics is designed for not exciting the unmodeled dynamics. Moura, Roy and Olgac [6] improved sliding mode control with perturbation estimation (SMCPE) by incorporating the above frequency-shaping features into the sliding function. For frequency shaping control design, Koshkouei and Zinober [2] proposed some new methods for designing the sliding surface and sliding mode control when the LQ weighting functions are not constant at all frequencies. Almost all the research works above, however, is limited to a PD type sliding surface. There have been no researches proposing the design method of an integral sliding surface, which

0-7803-7896-2/03/$17.00 ©2003 IEEE

Proceedings of the American Control Conference
Denver, Colorado June 4-6, 2003

should be used in TDCSA, using frequency-shaping approach.

In this paper, we propose the suitable integral sliding surface design method using frequency-shaping features for TDCSA. By incorporating frequency-shaping LQ design techniques into the integral sliding surface, the performance of TDCSA is more improved. TDCSA using a frequency-shaped integral sliding surface is shown to be a viable strategy for dynamics structures with unmodeled dynamics as well as dynamics uncertainties. Tests are conducted on a single-link flexible arm.

This paper is structured as follows. Section 2 will briefly introduce TDCSA law. In Section 3, we will propose the design method of the frequency-shaped integral sliding surface. Experimental results verifying the effectiveness of the proposed frequency-shaped integral sliding surface will be presented in Section 4

2. Time Delay Control with Switching Action (TDCSA)

In this section, TDCSA will be briefly introduced and the stability of TDCSA using an integral sliding surface will be analyzed.

2.1 TDCSA [3, 4]

The class of plants we are concerned with can be expressed in the following nonlinear differential equation:

$$\dot{\mathbf{x}}(t) = \mathbf{f}(\mathbf{x},t) + \mathbf{B}(\mathbf{x},t)\mathbf{u}(t) + \mathbf{d}(t), \quad (1)$$

where $\mathbf{x}(t) \in R^n$ denotes the state vector of the plant, $\mathbf{u}(t) \in R^r$ the control input vector, $\mathbf{f}(\mathbf{x},t) \in R^{n\times 1}$ the nonlinear function in companion form, which may be unknown; $\mathbf{d}(t) \in R^{n\times 1}$ unknown disturbances; and $\mathbf{B}(\mathbf{x},t) \in R^{n\times r}$ the control distribution matrix, the range of which should be known. In this plant, it is assumed that the states and their derivatives are measurable. If we select a constant matrix $\bar{\mathbf{B}}$ which is located within the known range of $\mathbf{B}(\mathbf{x},t)$ and use $\bar{\mathbf{B}}$, Eq. (1) is rearranged into the following:

$$\dot{\mathbf{x}}(t) = \bar{\mathbf{B}}\mathbf{u}(t) + \mathbf{H}(t), \quad (2)$$

where $\mathbf{H}(t)$ consists of terms representing uncertainties and time-varying factors, which are expressed as

$$\mathbf{H}(t) = \mathbf{f}(\mathbf{x},t) + \{\mathbf{B}(\mathbf{x},t) - \bar{\mathbf{B}}\}\mathbf{u}(t) + \mathbf{d}(t). \quad (3)$$

In addition, $\mathbf{H}(t)$ must be satisfied with the following matching condition

$$(\mathbf{I} - \bar{\mathbf{B}}\bar{\mathbf{B}}^+)(\dot{\mathbf{x}}_d - \mathbf{A}_m\mathbf{e} - \mathbf{H}) = 0. \quad (4)$$

TDCSA consists of Time Delay Control (TDC) and switching action of SMC. TDC makes, on the one hand, the plant accurately follow a desired error dynamics in the presence of unknown dynamics and unexpected disturbance. On the other hand, the switching action keeps the tracking error on the sliding surface so that the controller consequently becomes robust. *The reason that the integral sliding surface* is used for switching action is to *match* the desired error dynamics of TDC with the derivative of the sliding surface. If the derivative of the sliding surface is not equal to the desired error dynamics, the switching action acts differently from TDC so that the control performance deteriorates.

The desired error dynamics is defined with a reference model as the following:

$$\dot{\mathbf{e}}(t) = \mathbf{A}_m\mathbf{e}(t), \quad (5)$$

where $\mathbf{e}(t) = \mathbf{x}_d(t) - \mathbf{x}(t) \in R^n$ is the tracking error vector, $\mathbf{x}_d \in R^n$ the desired trajectory vector, and $\mathbf{A}_m \in R^{n\times n}$ a constant matrix of the desired error dynamics.

The TDC law that meets the desired error dynamics (Eq. (5)) is obtained as

$$\mathbf{u}_{tdc}(t) = \bar{\mathbf{B}}^+[\dot{\mathbf{x}}_d(t) - \hat{\mathbf{H}}(t) - \mathbf{A}_m\mathbf{e}(t)], \quad (6)$$

where $\bar{\mathbf{B}}^+$ denotes a pseudo-inverse of $\bar{\mathbf{B}}$ ($\bar{B}^+ = (\bar{B}^T\bar{B})^{-1}\bar{B}^T$)d and $\hat{\mathbf{H}}(t)$ the estimate of $\mathbf{H}(t)$. If L is very small and $\mathbf{H}(t)$ does not vary largely during the L times, the estimated $\hat{\mathbf{H}}(t)$ can be obtained by using both Eq. (2) and the fact that $\mathbf{H}(t)$ is usually a continuous function. More specifically, when L is small enough, then

$$\hat{\mathbf{H}}(t) \approx \mathbf{H}(t-L) = \dot{\mathbf{x}}(t-L) - \bar{\mathbf{B}}\mathbf{u}(t-L). \quad (7)$$

Combining Eq. (7) with Eq. (6), the TDC law is obtained as follows:

$$\mathbf{u}_{tdc}(t) = \mathbf{u}_{tdc}(t-L) + \bar{\mathbf{B}}^+[\dot{\mathbf{x}}_d(t) - \dot{\mathbf{x}}(t-L) - \mathbf{A}_m\mathbf{e}(t)]. \quad (8)$$

More details about the stability condition and the design of TDC can be found in [8].

L should be sufficiently small enough for TDC to meet the desired error dynamics of Eq. (5). The value used for L, however, is set to be that of the sampling time when TDC is implemented in a real-time controller. Therefore, the variation of system nonlinearities and disturbances occurring during the time delay (L), cause time delay estimation (TDE) error as follows:

$$\mathbf{H}(t) - \hat{\mathbf{H}}(t) = \mathbf{H}(t) - \mathbf{H}(t-L) = \Delta\mathbf{H}(t). \quad (9)$$

Because of the TDE error, TDC does not have the desired error dynamics of Eq.(5), but the following error dynamics:

$$\dot{\mathbf{e}}(t) = \mathbf{A}_m\mathbf{e}(t) - \bar{\mathbf{B}}\bar{\mathbf{B}}^+\Delta\mathbf{H}(t). \quad (10)$$

In order to match the desired error dynamics (Eq. (5)) with the sliding surface ($\mathbf{s}(t) = 0$), we use the integral sliding surface as follows:

$$\mathbf{s}(t) = \bar{\mathbf{B}}^+\int_0^t [\dot{\mathbf{e}}(\tau) - \mathbf{A}_m\mathbf{e}(\tau)]d\tau, \quad (11)$$

where the sliding surface has the initial value of zero ($\mathbf{s}(t=0) = 0$) and its derivative (Eq. (12)) is equal to the desired error dynamics (Eq. (5)).

$$\dot{\mathbf{s}}(t) = \bar{\mathbf{B}}^+[\dot{\mathbf{e}}(t) - \mathbf{A}_m\mathbf{e}(t)]. \quad (12)$$

Finally, the TDCSA is proposed by adding the switching action to TDC, as follows:

$$\mathbf{u}(t) = \mathbf{u}(t-L) + \bar{\mathbf{B}}^{+}[\dot{\mathbf{x}}_d(t) - \dot{\mathbf{x}}(t-L) - \mathbf{A}_m\mathbf{e}(t)] + \mathbf{K}\mathrm{sgn}(\mathbf{s}(t)) \quad (13)$$

where $\mathbf{K} \in R^{r\times r}$ denotes a switching gain matrix, which is obtained from the following stability condition: $\mathbf{s} \in R^r$, the sliding surface vector.

2.2 Stability Analysis of TDCSA

For the stability analysis of the overall system, the second method of Lyapunov is used. If the Lyapunov function is selected as $\mathbf{V} = \mathbf{s}^T\mathbf{s}/2$, its time derivative is as follows,

$$\begin{aligned}
\dot{\mathbf{V}} &= \mathbf{s}^T\dot{\mathbf{s}} = \mathbf{s}^T\bar{\mathbf{B}}^{+}[\dot{\mathbf{e}}(t) - \mathbf{A}_m\mathbf{e}(t)] \\
&= \mathbf{s}^T\bar{\mathbf{B}}^{+}[\dot{\mathbf{x}}_d(t) - \bar{\mathbf{B}}\mathbf{u}(t) - \mathbf{H}(t) - \mathbf{A}_m\mathbf{e}(t)] \\
&= \mathbf{s}^T\bar{\mathbf{B}}^{+}[\dot{\mathbf{x}}_d(t) - \bar{\mathbf{B}}\{\bar{\mathbf{B}}^{+}(\dot{\mathbf{x}}_d(t) - \hat{\mathbf{H}}(t) - \mathbf{A}_m\mathbf{e}(t)) \\
&\quad + \mathbf{K}\mathrm{sgn}(\mathbf{s})\} - \mathbf{H}(t) - \mathbf{A}_m\mathbf{e}(t)] \\
&= \mathbf{s}^T\bar{\mathbf{B}}^{+}[(\mathbf{I} - \bar{\mathbf{B}}\bar{\mathbf{B}}^{+})\{\dot{\mathbf{x}}_d(t) - \mathbf{A}_m\mathbf{e}(t) - \mathbf{H}(t)\} \\
&\quad - \bar{\mathbf{B}}\bar{\mathbf{B}}^{+}\Delta\mathbf{H}(t) - \bar{\mathbf{B}}\mathbf{K}\mathrm{sgn}(\mathbf{s})] \\
&= \mathbf{s}^T[-\bar{\mathbf{B}}^{+}\Delta\mathbf{H}(t) - \mathbf{K}\mathrm{sgn}(\mathbf{s})]
\end{aligned} \quad (14)$$

Therefore, the following condition is needed so that the time derivative of the Lyapunov function should be negative definite:

$$(K)_{ii} > \left|(\bar{B}^{+}\Delta H)_i\right| \text{ for } i = 1,\ldots,r. \quad (15)$$

In other words, the magnitude of the switching gain ($\mathbf{K}$) must be larger than that of the term due to the TDE error.

3. Frequency-Shaped Integral Sliding Surface

In this section, we will propose integral sliding surface using frequency-shaping features for TDCSA, by incorporating frequency-shaping LQ design techniques [1] into the integral sliding surface.

3.1 Frequency-shaped integral sliding surface

The design method of a frequency-shaped integral sliding surface is presented below. A general second-order system is taken for simplicity. However, the technique is easily expandable to arbitrary order

Let define the cost function using frequency dependent weighting matrices

$$J = \int_{-\infty}^{+\infty}\left\{[Q_j(w)e_j(w)]^2 + Q_l q_i^2(w) + \dot{e}_j^2(w)\right\}dw \quad (16)$$

where $e_j = x_{jd}(t) - x_j(t)$ and $\dot{e}_j = \dot{x}_{jd}(t) - \dot{x}_j(t)$ is tracking error and tracking velocity error, respectively; $q_j = \int_0^t e_j(t)dt$ is the integral value of e_j; and $Q_l \geq 0$ is a weighting value for q_j. If we choose $Q_j(w)$ to have low-pass characteristics and set Q_l to be zero, the minimization of J will penalize high-frequency components on the state ($e_j, \dot{e}_j$). This is true since $Q_j(w)$ is reduced at high frequencies, consequently $\dot{e}_j^2$ terms become dominant.

If we define Q_l to be over zero, the integral term (q_j) have equal weighting for all frequencies. The time domain equivalent of Eq. (16) is given as

$$J = \int_0^{\infty}[y_j^2(t) + Q_l q_j^2(t) + \dot{e}_j^2(t)]dt \quad (17)$$

where $y_j(t)$ is the output of a n_j-order filter defined by $Q_j(w)$ with e_j as the input. The following is the state-space representation of this input-output relation:

$$\begin{aligned}
\dot{\mathbf{z}}_j(t) &= \mathbf{F}_j\mathbf{z}_j(t) + \mathbf{G}_j e_j(t) \\
y_j(t) &= \mathbf{\Phi}_j\mathbf{z}_j(t) + \mathbf{D}_j e_j(t)
\end{aligned} \quad (18)$$

where $\mathbf{z}_j \in R^{n_j}$ is the filter state vector and $\mathbf{F}_j, \mathbf{G}_j, \mathbf{\Phi}_j, \mathbf{D}_j$ have corresponding dimensions. Eq. (17) can be rewritten as

$$J = \int_0^{\infty}\left\{\mathbf{w}_{1j}^T\mathbf{Q}\mathbf{w}_{1j} + w_{2j}^T w_{2j}\right\}dt \quad (19)$$

where

$$\mathbf{w}_{1j} = \begin{bmatrix}\mathbf{z}_j^T & q_j & e_j\end{bmatrix}^T$$

$$w_{2j} = \dot{e}_j$$

$$\mathbf{Q} = \begin{bmatrix}\mathbf{\Phi}_j^T\mathbf{\Phi}_j & \mathbf{0} & \mathbf{\Phi}_j^T\mathbf{D}_j \\ \mathbf{0} & \mathbf{Q}_l^T\mathbf{Q}_l & \mathbf{0} \\ \mathbf{D}_j^T\mathbf{\Phi}_j & \mathbf{0} & \mathbf{D}_j^T\mathbf{D}_j\end{bmatrix}$$

Note that $\mathbf{w}_{1j}$ and w_{2j} are related through the linear time invariant (LTI) system

$$\begin{aligned}
\dot{\mathbf{w}}_{1j} &= \mathbf{A}\mathbf{w}_{1j} + \mathbf{B}w_{2j} \\
\text{where } \mathbf{A} &= \begin{bmatrix}\mathbf{F}_j & \mathbf{0} & \mathbf{G}_j \\ \mathbf{0} & \mathbf{0} & \mathbf{1} \\ \mathbf{0} & \mathbf{0} & \mathbf{0}\end{bmatrix}, \mathbf{B} = \begin{bmatrix}\mathbf{0} \\ \mathbf{0} \\ \mathbf{1}\end{bmatrix}
\end{aligned} \quad (20)$$

The conventional optimal solution to the LQR problem of Eq. (19) and Eq. (20) is

$$\begin{aligned}
w_{2j} &= -\mathbf{K}_j\mathbf{w}_{1j} \\
\text{where } \mathbf{K}_j &= \mathbf{A}_{2j}^T\mathbf{T}
\end{aligned} \quad (21)$$

where T is the solution of the Riccati equation

$$\mathbf{T}\mathbf{A}_{1j} + \mathbf{A}_{1j}^T\mathbf{T} - \mathbf{T}\mathbf{A}_{2j}\mathbf{A}_{2j}^T\mathbf{T} + \mathbf{Q} = \mathbf{0} \quad (22)$$

Eq. (21) expresses the desired relation among the state variables, which is satisfied by defining

$$s_j = \dot{e}_j + \mathbf{K}_j\begin{bmatrix}\mathbf{z}_j \\ q \\ e_j\end{bmatrix} = \dot{e}_j + \mathbf{H}_j\mathbf{z}_j + K_1 q + K_2 e_j \quad (23)$$

and forcing the system to stay on $s_j = 0$.

3.2 TDCSA using Frequency-shaped Integral Sliding Surface

The desired error dynamics is obtained from the relation between the desired error dynamics of TDC and the integral sliding surface – the derivative of the sliding surface is equal to the desired error dynamics.

$$\ddot{e}_j + K_2\dot{e}_j + K_1 e_j + \mathbf{H}_j\dot{\mathbf{z}}_j = 0$$

$$\text{or} \quad \begin{bmatrix}\dot{e}_j \\ \ddot{e}_j\end{bmatrix} = \begin{bmatrix}0 & 1 \\ -K_1 & -K_2\end{bmatrix}\begin{bmatrix}e_j \\ \dot{e}_j\end{bmatrix} + \begin{bmatrix}0 \\ H_{j1} \quad \cdots \quad H_{jn}\end{bmatrix}\begin{bmatrix}\dot{z}_1 \\ \vdots \\ \dot{z}_n\end{bmatrix} \tag{24}$$

Using Eq. (23) and Eq. (24), the TDCSA using frequency-shaped integral sliding surface is obtained as

$$\mathbf{u}(t) = \mathbf{u}(t-L) + \bar{\mathbf{B}}^{+}[\dot{\mathbf{x}}_d(t) - \dot{\mathbf{x}}(t-L) - \mathbf{A}_m\mathbf{e}(t) + \mathbf{H}\dot{\mathbf{z}}(t)] + \mathbf{K}\mathrm{sgn}(\mathbf{s}(t)) \tag{25}$$

where

$$\mathbf{s}(t) = \begin{bmatrix}s_1 \\ \vdots \\ s_r\end{bmatrix}, \mathbf{z}(t) = \begin{bmatrix}\mathbf{z}_1^T & \cdots & \mathbf{z}_r^T\end{bmatrix}, \mathbf{H} = \begin{bmatrix}0 \\ \mathbf{H}_1 \quad \cdots \quad \mathbf{H}_r\end{bmatrix}$$

4. Experiment

To verify the effectiveness of the proposed frequency-shaped integral sliding surface, experiments were performed on a single-link flexible arm like as Fig. 1.

4.1 Single-link flexible arm

This single-link flexible arm consists of a flexible arm, a following arm, a linear guide, two encoders and a motor. The material of the flexible arm is spring steel plate. The following arm is located over the flexible arm to measure the tip displacement of the flexible arm relative to the angle of motor. Encoder 2 senses the angle of the following arm and detects the tip displacement. The linear guide, connecting with the following arm and the flexible arm, is located to minimizes the friction force and prevent the warp of the flexible arm.

The single-link flexible arm used at this experiment can be modeled simply as clamp-free model as shown in Fig. 2. The mathematical model of this arm can be derived by using the assumed mode method associated with Lagrangian formulation [5]. If first flexible mode is only considered, the approximated mathematical model of this arm is

$$\begin{bmatrix}M_{11} & M_{12} \\ M_{21} & M_{22}\end{bmatrix}\begin{bmatrix}\ddot{\theta}_1 \\ \ddot{\theta}_2\end{bmatrix} + \begin{bmatrix}g_1(\dot{\theta}_1,\theta_2,\dot{\theta}_2) \\ g_2(\dot{\theta}_1,\theta_2)\end{bmatrix} + \begin{bmatrix}0 \\ k\theta_2\end{bmatrix} = \begin{bmatrix}\tau \\ 0\end{bmatrix} \tag{26}$$

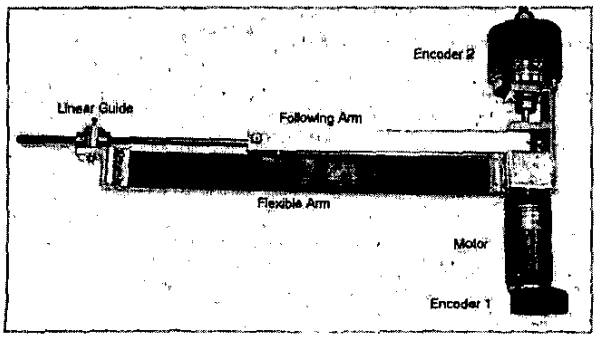

Figure 1 : Experimental setup of single-link flexible arm

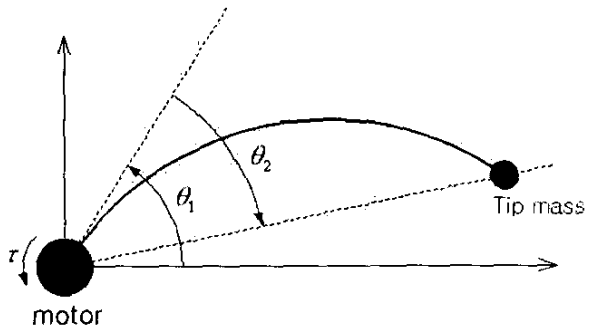

Figure 2 : Clamp-free model of flexible arm

where θ_1 and θ_2 are the angles of motor and tip, respectively, as shown in Fig. 2; k is time-varying spring coefficient; g_i is viscous term; M_{ij} is inertial term and τ is the motor's torque.

4.2 Controller Design

Given the desired trajectory about the angle of motor (θ_1), the control objective is to control the angle of motor while keeping $|\theta_2|$ as small as possible. We assume that the flexible arm is rigid.

Now we consider a reduced order one-link model of the flexible arm as follows:

$$\bar{M}\ddot{\theta}_1 + H(t) = \tau \tag{27}$$

where $\bar{M}$ is a constant value representing the known range of $M_{11}(\theta_2)$, whereas $H(t)$ consists of terms representing uncertainties and time-varying factors.

For Eq. (27), without considering the resonance mode, original TDCSA law is obtained as follows:

$$u(t) = u(t-L) - \bar{M}\ddot{\theta}_1(t-L) + K\,\mathrm{sgn}(s(t)) + \bar{M}[\ddot{\theta}_d(t) + K_v(\dot{\theta}_d - \dot{\theta}_1) + K_p(\theta_d - \theta_1)] \tag{28}$$

where

$s(t) = \dot{e}(t) + K_v e(t) + K_p\int e(t)dt - \dot{e}(t=0) - K_v e(t=0)$, the value of gains are selected: $\bar{M} = 0.00011$, $K_v = 6$, $K_p = 9$, and $K = 0.001$.

For step input ($\theta_d = -60°, \dot{\theta}_d = \ddot{\theta}_d = 0$), original TDCSA is applied to the single-link flexible arm. Fig. 3 shows the response of the flexible arm to the step input. Fig. 4 shows the power spectral density of θ_2. As shown in Fig. 4, the unmodeled flexible mode is located at 0.7 Hz. Because this unmodeled flexible mode, the oscillation exists in the response of θ_2 (Fig. 3 (c)). This oscillation affects the response of θ_1, as shown in Fig. 3 (a) and (b). The unmodeled mode drops the overall control performance.

In order that the flexible mode excitation is minimized, now we design a frequency-shaped integral sliding surface. The peak frequency of unmodeled dynamics is 0.7Hz (Fig. 4). Firstly the cost function filter (Q_j of Eq. (16)) is selected as

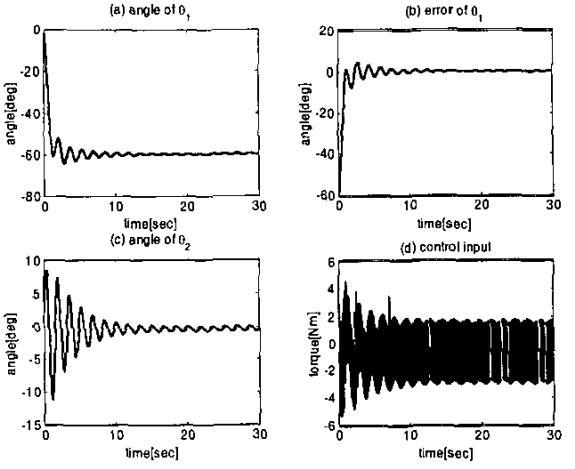

Figure 3 : Step response of the flexible arm using original TDCSA

$$Q_1(p)=\frac{374.20}{p^4+11.49p^3+66.04p^2+222.32p+374.20} \quad (29)$$

which is 4th butterworth filter having the cut-off frequency of 0.7Hz. The state-space representation of $Q_1(p)$ defines $\mathbf{F}_1$, $\mathbf{G}_1$, $\mathbf{\Phi}_1$, and $\mathbf{D}_1$. The weighting value (Q_1 of Eq. (16)) for integral error ($q = \int e(t)dt$) is selected to be 3 [rad/s]. Following section 3.1, the frequency-shaped sliding surface is

$$\begin{aligned} s^*(t) &= \dot{e}(t) + 2.573e(t) + 3.0\int e(t)dt \\ &+0.310z_1(t) + 3.153z_2(t) + 13.688z_3(t) \\ &+25.513z_4(t) - \dot{e}(0) - 2.573e(0) \end{aligned} \quad (30)$$

From Eq. (30), the desired error dynamics is obtained as follows:

$$\begin{aligned} &\ddot{e}(t) + 2.573\dot{e}(t) + 3.0e(t) + 0.310\dot{z}_1 \\ &+3.153\dot{z}_2 + 13.688\dot{z}_3 + 25.513\dot{z}_4 = 0 \end{aligned} \quad (31)$$

By using Eq. (30) and Eq. (31), TDCSA using

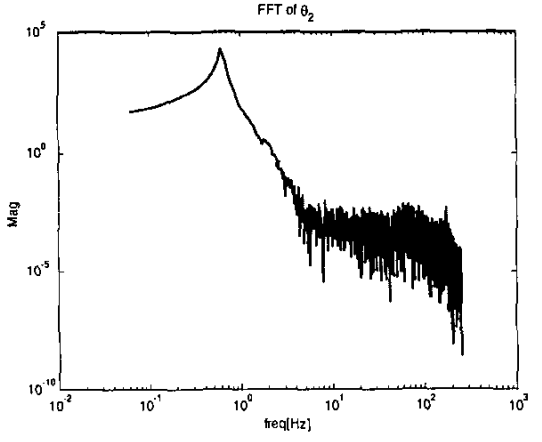

Figure 4 : Power spectral density of θ_2

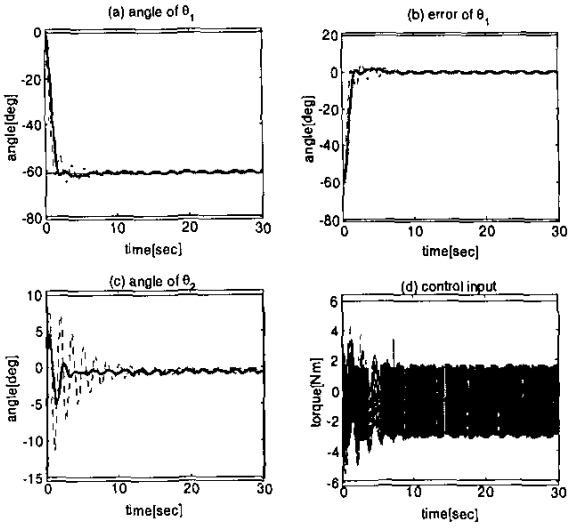

Figure 5 : Experimental results for step input (solid line stands for TDCSA using a frequency-shaped integral sliding surface; and dotted line for original TDCSA)

frequency-shaped integral sliding surface is obtained as follows:

$$\begin{aligned} u(t) &= u(t-L) - \bar{M}\ddot{\theta}_1(t-L) + \bar{M}[\ddot{\theta}_d(t) \\ &+2.573\dot{e}(t) + 3.0e(t) + 0.310\dot{z}_1 + 3.153\dot{z}_2 \\ &+13.688\dot{z}_3 + 25.513\dot{z}_4] + K\,\mathrm{sgn}(s^*(t)) \end{aligned} \quad (32)$$

Fig. 5 shows the step responses of the flexible arm with TDCSA using a frequency-shaped integral sliding surface. Fig. 6 shows the power spectral density of θ_2. In comparison with the responses using original TDCSA (dotted line), the oscillation of θ_1 and θ_2 is reduced. As shown in Fig. 6, the excitation of the first flexible mode at 0.7Hz is suppressed. Accordingly, the above experiment results show that the frequency-shaped sliding surface can avoids the excitation of the first flexible mode.

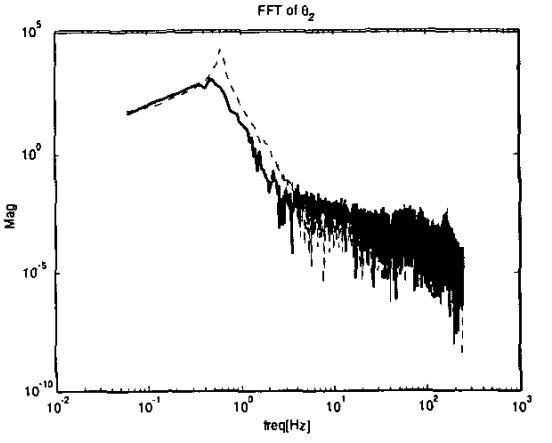

Figure 6 : Power spectral density of θ_2 (solid line stands for TDCSA using a frequency-shaped integral sliding surface; and dotted line for original TDCSA)

5. Conclusion

When TDCSA is applied to nonlinear system having high frequency resonance modes, undesired vibration or chattering is occurred. This problem results from the switching action and high gains. Fast sliding mode dynamics or fast desired error dynamics improve the control performance, but excite the unmodeled resonance modes and cause undesired vibration or chattering. To suppress this undesired vibration or chattering, we proposed the integral sliding surface design method, which is suitable for TDCSA, by using frequency-shaping features. This method is to incorporate frequency-shaping LQ design techniques into an integral sliding surface.

By experimental results, the frequency-shaped integral sliding surface is shown to be a practicable for a single-link flexible arm. Motion control of a single-link flexible arm with a unmodeled flexible modes is taken into account. The desired trajectory is tracked while minimally exciting the unmodeled flexible modes.

This design method of a frequency-shaped integral sliding surface will be useful to SMC using an integral sliding surface.

References

[1] Gupta, N. K., 1980, "Frequency-shaped cost functionals: Extension of linear-quadratic-Gaussian design methods," *Journal of Guidance and Control*, vol. 3, no. 6, pp. 529-535.

[2] Koshkouei, A. Jafari and Zinober, A.S.I., 2000, "Robust frequency shaping sliding mode control," IEE proceedings D, Control theory and applications, Vol. 147, No. 3, pp. 312-320.

[3] Lee, S. U. and Chang, P. H., 2002, "Control of a heavy-duty robotic excavator using Time Delay Control with Integral Sliding Surface," Control Engineering Practice, Vol. 10, Iss. 7, pp. 697-711.

[4] Lee, S. U. and Chang, P. H., 2002, "The Development of Anti-Windup Scheme for Time Delay Control with Switching Action Using Integral Sliding Surface," Transactions of the KSME (A), Vol. 26, No. 8, pp. 1534-1544.

[5] Luca, A. D. and Siciliano, B., 1988, "Joint-Based Control of a Nonlinear Model of a Flexible Arm," Proc. *of American Control Conference*, pp. 965-940.

[6] Moura, J. T., Roy, R. G. and Olgac, N., 1997, "Frequency-Shaped Sliding Modes: Analysis and Experiments," IEEE Transactions on Control Systems Technology, Vol. 5, No. 4, pp. 394-401.

[7] Slotine, J.-J. E. and Li, W., 1991, Applied Nonlinear Control, Prentice-Hall International Editions.

[8] Youcef-Toumi, K. and Ito, O., 1990, "A Time Delay Controller for Systems with Unknown Dynamics," ASME Journal of Dynamic System, Measurement and Control, Vol. 112, pp. 133-141

[9] Young K. D. and Özgüner, Ü., 1993, "Frequency shaping compensator design for sliding mode," International Journal of Control, Vol. 57, No. 5, pp. 1005-1019.